BIOLOGY OF REPRODUCTION **82,** 669–678 (2010)
Published online before print 30 December 2009.
DOI 10.1095/biolreprod.109.079566

The Annulus of the Mouse Sperm Tail Is Required to Establish a Membrane Diffusion Barrier That Is Engaged During the Late Steps of Spermiogenesis[1]

Susanna Kwitny,[3] Angela V. Klaus,[4] and Gary R. Hunnicutt[2,3]

Population Council,[3] Center for Biomedical Research, Rockefeller University, New York, New York
Department of Biological Sciences,[4] Seton Hall University, South Orange, New Jersey

ABSTRACT

The annulus is a higher order septin cytoskeletal structure located between the midpiece and principal piece regions of the sperm tail. The annulus has been hypothesized to generate the diffusion barrier that exists between these two membrane domains. We tested this premise directly on septin 4 knockout mice, whose sperm are viable but lack an annulus, by following the diffusing membrane protein basigin. Basigin is normally confined to the principal piece domain on testicular and caput sperm, but undergoes relocation into the midpiece during sperm epididymal transit. On *Sept4*$^{-/-}$ sperm, domain confinement was lost, and basigin localized over the entire plasma membrane. Both immunofluorescence and immunoblotting further revealed reduced levels of basigin expression on sperm from the knockout. Testicular immunohistochemistry showed similar basigin expression and tail targeting in wild-type (WT) and *Sept4*$^{-/-}$ tubules until step 15 of spermatid development, at which point basigin was redistributed throughout the plasma membrane of *Sept4*$^{-/-}$ spermatids. The basigin outside of the tail was subsequently lost around the time of sperm release into the lumen. The redistribution in the knockout coincides with the time in WT sperm when the annulus completes its migration from the neck down to the midpiece-principal piece junction. We posit that basigin may not diffuse freely until after the annulus arrives at the midpiece-principal piece junction to restrict lateral movement. These results are the strongest evidence to date of a mammalian septin structure establishing a membrane diffusion barrier.

annulus, gamete biology, gametogenesis, sperm, sperm maturation

INTRODUCTION

Sperm leave the testes as highly compact, streamlined cells specialized for traveling great distances. Lacking any protein synthetic machinery, they are preloaded with a vast array of proteins that are needed at different times and in different environments leading up to fertilization [1]. Sperm use a variety of methods to precisely regulate when and how each protein will be activated. These include posttranslational modifications, interactions with secreted epididymal proteins, and, of particular interest here, the sequestration and redistribution of proteins within and between defined membrane domains.

The selective mixing and shuffling of proteins between domains likely sets up coordinated protein interactions and induces specific signaling pathways that culminate in functional changes. Such rearrangements have been correlated with the acquisition of motility, hypermotility, capacitation, the acrosome reaction, and the sperm-egg interaction of fertilization [2–11]. Presumably, early domain segregation of many proteins ensures that the above events do not proceed prematurely. Protein sequestration may also protect sperm against protein loss. For example, ADAM1/ADAM2 (fertilin) and SPAM1 (PH-20) are both found over the whole head of testicular guinea pig sperm, however, they both become localized within the posterior head domain during epididymal maturation [4, 12, 13]. Without this redistribution, the ADAM1/ADAM2 and SPAM1 proteins located over the anterior head would be lost as that membrane is shed during the acrosome reaction. This could be functionally catastrophic for the sperm.

Confinement of proteins within membrane domains has been documented on the sperm tail as well [14–18]. The two major tail membrane domains are the principal piece and the midpiece, and between these regions lies a cytoskeletal structure called the annulus (Fig. 1). The annulus has long been speculated to have a role in maintaining these discrete tail domains. Freeze fracture analysis of the membrane above the annulus reveals organized and densely packed circumferential arrays of membrane proteins, which could function as a kind of physical barrier to lateral diffusion [19, 20]. Fluorescence redistribution after photobleaching studies have also identified proteins that are freely diffusing within the membrane and yet remain confined within sperm tail domains [14, 16]. To date, however, no direct evidence for annulus involvement has been established.

Interestingly, the midpiece-principal piece barrier can act as a gated fence, allowing the translocation of selected proteins at prescribed times. The membrane proteins basigin (rat and mouse) and PT-1 (guinea pig) are both freely diffusing but confined to the principal piece domain on caput epididymal sperm. Basigin, however, redistributes by moving into the midpiece during sperm maturation in the epididymis [16–18]. PT-1 similarly relocalizes to the midpiece, but not until the time of sperm capacitation [14]. It is hypothesized that the timing of each protein's redistribution is in some way related to its functional activity. Little is known about PT-1, but basigin (EMMPRIN, CE9, CD147, MC31) is a transmembrane glycoprotein belonging to the immunoglobulin superfamily. Its function on mature sperm is unknown because basigin knockout mice have spermatogenesis arrested at metaphase of the first meiotic division [21].

Previously, we and others showed that the sperm annulus is a septin-ringed structure composed of septin family members 1, 4, 6, 7, and 12 [22–24]. When the gene for septin 4 is knocked

[1]Supported by the National Institute of Health research grant HD038807.
[2]Correspondence: Gary R. Hunnicutt, Population Council, 1230 York Ave., New York, NY 10065. FAX: 212 327 7678;
e-mail: ghunnicutt@popcbr.rockefeller.edu

Received: 22 June 2009.
First decision: 23 July 2009.
Accepted: 23 December 2009.

eISSN: 1529-7268 http://www.biolreprod.org
ISSN: 0006-3363

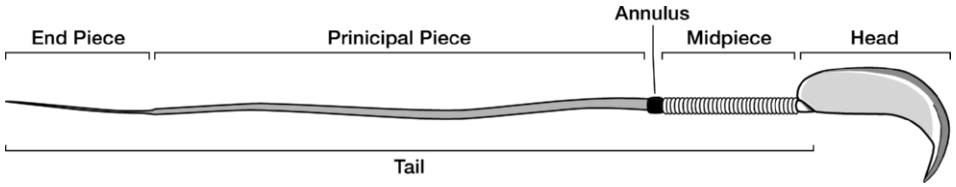

FIG. 1. A cartoon of a mature sperm showing the location of the cytoskeletal annulus with relationship to the various domains of the sperm tail.

out of mice, the males produce sperm devoid of an annulus [22, 23]. These sperm are viable but do not swim and are infertile. Septins are a conserved family of polymerizing GTP-binding proteins associated with diverse processes in dividing and nondividing cells [25–30]. Interestingly, septin rings were first discovered in yeast at the mother-daughter budding site, where septin collars appear to function as diffusion barriers that maintain a polarized state between the mother and growing daughter cells [31–39]. This type of role has been suggested for septin structures in other cellular systems as well [40–42].

In this study, we establish the first direct evidence for the role of the annulus in maintaining sperm membrane domains. Using basigin as a representative diffusing membrane protein, we examined its distribution from spermatogenesis through epididymal maturation on sperm from wild-type (WT) and *Sept4*$^{-/-}$ mice. We hypothesized that if the septin-comprised sperm annulus does act as a diffusion barrier, then sperm lacking an annulus should no longer show distinct tail membrane domain localizations for basigin.

MATERIALS AND METHODS

Animals

All the mice used in this study had C57BL/6 genetic backgrounds and were at least 12 wks old. All procedures were reviewed and approved by the Institutional Animal Care and Use Committee of The Rockefeller University and were performed in accordance with the Guide for the Care and Use of Laboratory Animals.

Isolation of Spermatozoa and Preparation of Testicular Tissues

Testicular sperm were isolated from surgically removed testes that were placed in modified Whitten medium (ModW; 22 mM Hepes, 1.2 mM $MgCl_2$, 100 mM NaCl, 4.7 mM KCl, 1.0 mM pyruvic acid, 5.5 mM glucose, 4.8 mM lactic acid, pH 7.3) with phenylmethanesulphonylfluoride (1 mM) immediately added. The capsule was removed and the seminiferous tubules minced to allow the testicular sperm to seep out. The material was then filtered through a 100 μm nylon mesh, layered over 7.5% Percoll-ModW, and spun at 1000 g_{av} for 10 min at 13°C. The pellet was resuspended in ModW, layered on a step gradient of 40% and 90% Percoll-ModW, and spun at 10 000 × *g* for 15 min at 13°C. The sperm layer was removed, diluted 1:10 in ModW, and respun at 500 × *g* as above. The testicular sperm pellet was resuspended in ModW.

Caput, corpus, and cauda epididymal sperm were isolated following dissection of these regions into ModW. Tissues were minced, and the expelled sperm from each was filtered through a 100 μm mesh [43]. Both the testicular and epididymal sperm concentrations were determined by doing cell counts using a hemocytometer.

Histological sections were prepared from whole testes that were dissected out of mice, immersed in Bouin fixative (71% picric acid, 24% formaldehyde, 5% glacial acetic acid), and incubated at room temperature (RT) overnight with gentle rotation. They were then transferred to the Rockefeller Comparative Biosciences Center where they were rinsed in 70% ethanol, embedded in paraffin blocks, and cut into sequential 4-μm sections that were mounted on slides.

Indirect Immunofluorescence

Sperm used in single labeling experiments were initially fixed with 3.7% formaldehyde for 30 min on ice, then washed into PBS, and stored at 4°C or dried onto slides and stored at −80°C until use. Sperm were incubated in a 1:500 dilution of a rabbit serum containing the polyclonal basigin antibody (gift from Dr. James Bartles, Northwestern University Medical School, Chicago, IL) for 1 h at 37°C. Negative controls were incubated in a 1:500 dilution of normal rabbit serum. Sperm were washed, then incubated in a 1:1000 dilution of AlexaFluor 546 goat anti-rabbit IgG (Invitrogen, http://www.invitrogen.com/site/us/en/home.html) secondary antibody for another hour at 37°C, and washed again before viewing with an epifluorescent microscope. The basigin localization pattern was quantified for caput and cauda sperm from WT and *Sept4*$^{-/-}$ mice. Micrographs of various fields of view were taken and contrast enhanced to reveal basigin's pattern of localization on dimly-labeled null sperm. All the sperm in each micrograph were recorded as either principal piece only, midpiece only, or other. More than 200 caput and 200 cauda sperm were counted from each of two WT mice and two *Sept4*$^{-/-}$ mice.

Double labeling of sperm was performed on freshly isolated sperm that were immediately fixed in formaldehyde and also on sperm that were initially flash frozen in liquid nitrogen and then formaldehyde-fixed immediately after thawing. Fixed sperm were incubated in 0.5% Triton X-100 in PBS for 20 min at RT, then pelleted and resuspended in a primary antibody mix consisting of rabbit anti-septin 4 (H-120) at 1:50 (Santa Cruz, http://www.scbt.com/) and rat anti-basigin (CD147) monoclonal antibody at 1:100 (eBioscience, http://www.ebioscience.com/) in PBS with 0.2% gelatin. Sperm were incubated for 1–2 h at 37°C or overnight at 4°C, pelleted, resuspended in PBS, and pelleted through 3% bovine serum albumin-PBS to remove unbound antibody. Sperm were then resuspended in a secondary antibody mix consisting of AlexaFluor 546 goat anti-rabbit IgG and FITC-conjugated goat anti-rat IgG (both Invitrogen) for 1 h at 37°C, washed again as above, and resuspended in PBS.

Single labeling of testicular tissue sections was performed both with the rabbit anti-basigin (polyclonal) antibody and the rabbit anti-septin 4 antibody at the concentrations described above. Before basigin labeling, sections were blocked with 10% normal goat serum (NGS) for 30 min at RT. Before septin 4 labeling, sections were subjected to heat-induced epitope retrieval (HIER) in addition to NGS blocking. HIER was done by placing the slides into 95°C Tris-ethylenediaminetetraacetic acid (EDTA) buffer (10 mM Tris base, 1 mM EDTA, 0.05% Tween 20, pH 9.0) for 20 min, followed by a 5-min PBS wash. Primary and secondary antibody incubations were each carried out for 1 h at 37°C, followed by 3 washes in PBS. The AlexaFluor 546 goat anti-rabbit secondary antibody was used with both labels. Slides bearing sequential sections were stained with hematoxylin and eosin for use in staging the labeled tubules.

Immunolabeled samples had cover slips affixed with ProLong Gold Antifade (Invitrogen) and were examined with an Olympus BX60 epifluorescence microscope equipped with filters for viewing fluorescein and rhodamine emissions. Images were acquired with an Olympus QImaging digital camera using QCapture 2.68.6 software (Quantitative Image Corporation, http://www.qimaging.com/) and imported into Adobe Photoshop 7.0 for analysis. For tissue sections, annulus and basigin labeling was captured with a 510–550 nm filter and converted to grayscale. A second picture was taken through a 450–480 nm filter, which caused the spermatid heads and midpieces to slightly autofluoresce. This image was converted to grayscale and inverted, causing the heads and midpieces to appear dark gray. The images were overlayed.

Immunoblots

Reduced and heated sperm samples were loaded at 10^5 cell equivalents/lane and resolved on 10% SDS-PAGE gels with protein standards before being transferred to polyvinylidene fluoride membranes for immunoblotting. Membranes were blocked in 5% nonfat dry milk in 10 mM Tris-buffered saline with 0.1% Tween-20 (TBS-T) and then probed with rabbit polyclonal anti-basigin antibody diluted 1:5000 in the blocking solution. The membranes were washed in three exchanges of TBS-T before incubating in peroxidase-conjugated secondary antibody for an hour at RT followed by three additional washes. Signal detection was achieved using ECL-Plus (GE Healthcare, http://www4.gelifesciences.com/aptrix/upp01077.nsf/Content/na_homepage). We confirmed the cell equivalent loads by stripping the immunoblots (0.7% beta mercaptoethanol, 2% SDS, 62.5 mM Tris, pH 6.8) and reprobing them for β-tubulin.

Cold-Field Emission Scanning Electron Microscopy

Isolated sperm were fixed in 2.5% glutaraldehyde, 0.1 M cacodylate buffer (pH 9) overnight at 4°C. A droplet of each sperm suspension was then placed

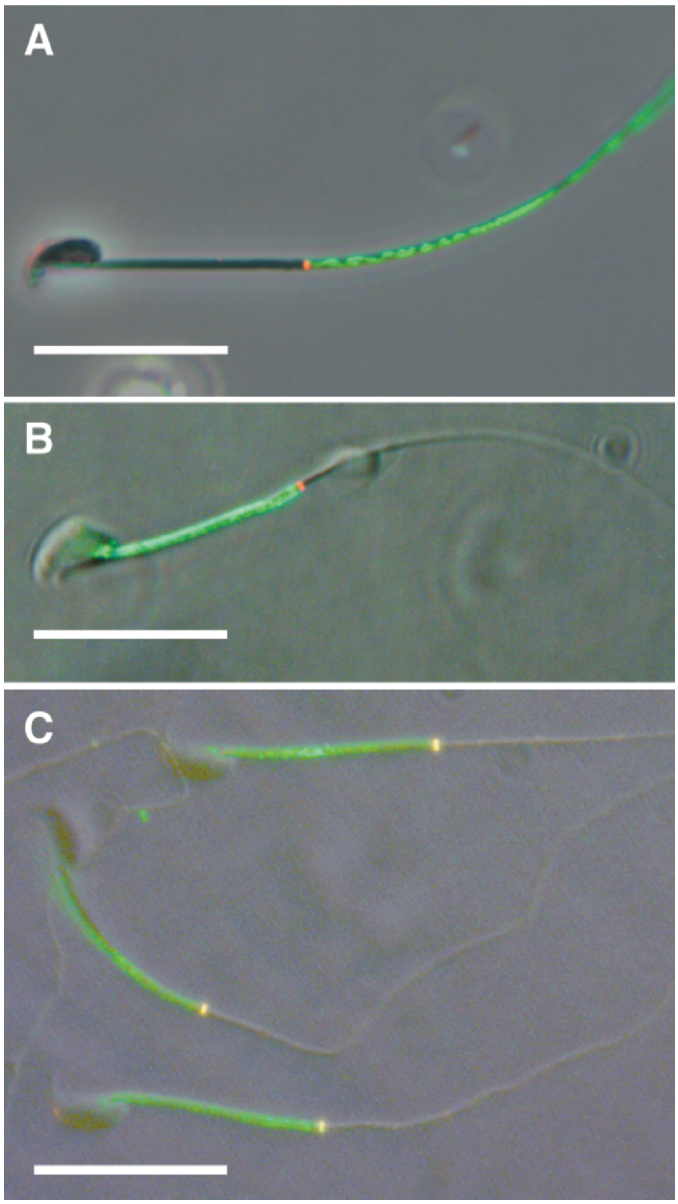

FIG. 2. Representative micrograph overlays of mouse caput (**A**) and cauda (**B** and **C**) epididymal sperm double labeled for basigin (green) and the annular protein septin 4 (red). Basigin labels the principal piece of caput sperm (**A**) and the midpiece of cauda sperm (**B**), stopping discretely at the annulus in both cases. Cauda sperm initially frozen and thawed before fixation (**C**) show coincident labeling for both proteins at the annulus (yellow). Bar = 20 μm.

on 12 mm round coverslips coated with 0.01% poly-L-lysine and allowed to adhere for 30 min at 4°C. Coverslips were rinsed by dipping in 0.1 M cacodylate buffer and dehydrated through an ethanol series (20%, 50%, 70%, 80%, 95%, 2 min each; 100%, two changes for 10 min each). Specimens were critical point dried (Oerlikon Balzers, http://www.oerlikon.com/balzers/), briefly sputter-coated (10–30 sec; Desk II, Denton Vacuum, http://www.dentonvacuum.com/equipment/Desk/Desk.html) with gold/palladium, and viewed in a Hitachi S-4700 cold-field emission scanning electron microscope operating at 5 kV accelerating voltage and 7 μA emission current. Images were collected digitally at 2560 × 1920 (512 pixels/inch) resolution.

RESULTS

The Annulus As a Domain Boundary in WT Sperm

We examined the relationship of basigin to the annulus during WT sperm maturation through indirect immunofluorescence. We colabeled WT caput and cauda epididymal sperm for the proteins basigin and septin 4, a marker for the annulus. We used monoclonal rat anti-basigin antibody and polyclonal rabbit anti-septin 4 antibody. As anticipated, basigin localized to the principal piece in caput sperm, immediately distal to the annulus, with little-to-no overlap (Fig. 2A). On cauda sperm, basigin localized to the midpiece, this time showing strict domain demarcation proximal to the annulus (Fig. 2B). However, we did note that if cauda sperm were fresh-frozen before fixation, then basigin also labeled on the membrane over the annulus, stopping in this case at the distal boundary of the annulus (Fig. 2C).

Failure of Annulus-Lacking Sperm to Uphold Membrane Domains

In order to determine if the annulus is required to establish and regulate the tail membrane domains, we took advantage of *Sept4*$^{-/-}$ mice, whose sperm lack the annulus [22, 23]. The lack of the annulus produces an interruption in the cytoskeleton at the midpiece-principal piece junction, as seen with scanning electron microscopy (Fig. 3), though the plasma membrane is presumably intact over this region. Using a polyclonal rabbit serum basigin antibody, we performed indirect immunofluorescence on isolated sperm from testes and the caput, corpus, and cauda epididymal regions. We found that sperm from *Sept4*$^{-/-}$ mice did not show typical membrane restriction of basigin, but instead displayed an unrestricted, whole-membrane distribution pattern at every stage. Table 1 shows data compiled from multiple experiments comparing WT and *Sept4*$^{-/-}$ sperm from the caput and cauda epididymis (before and after basigin relocalizes on WT sperm). *Sept4*$^{-/-}$ sperm demonstrated no change in labeling pattern. Basigin similarly labeled the whole membrane on *Sept4*$^{-/-}$ corpus sperm, during which stage basigin on WT sperm shows multiple distribution patterns as it transitions from the principle piece to the

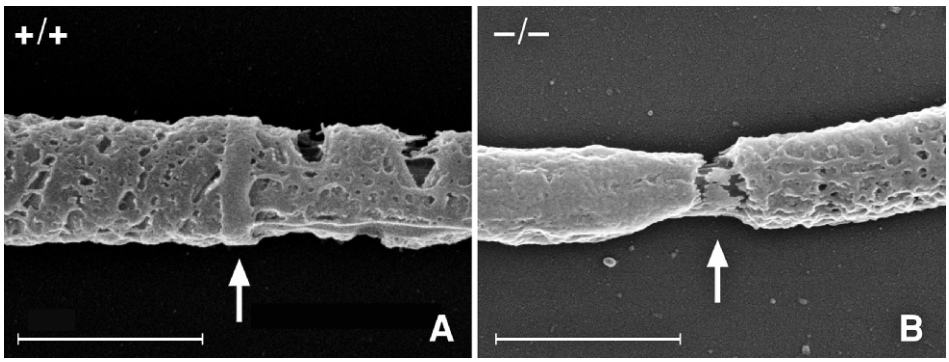

FIG. 3. Cold-field emission scanning electron micrographs of demembranated sperm tails focusing on the principal piece-midpiece junction. **A**) shows the annulus (arrow) of a WT sperm, while **B** shows the gap (arrow) created by the missing annulus of a *Sept4*$^{-/-}$ sperm. In both pictures, the mitochondrial sheath of the midpiece is to the left of the arrow, and the fibrous sheath of the principal piece is to the right of the arrow. Bar = 1.0 μm.

TABLE 1. Quantification of epididymal sperm from WT and *Sept4*$^{-/-}$ mice showing basigin localization after indirect immunofluorescence visualization.

Sperm genotype and source	Principal piece only (%)	Midpiece only (%)	No domain restrictions (%)	No signal detected (%)
Caput				
WT	87.7	0.0	4.5	7.8
Sept4$^{-/-}$	4.9	0.0	95.1	0.0
Cauda				
WT	2.8	80.3	8.6	8.3
Sept4$^{-/-}$	0.0	0.7	96.4	2.9

midpiece (data not shown). Testicular sperm appeared similar to caput sperm for both genotypes.

Additionally, epididymal sperm from *Sept4*$^{-/-}$ mice displayed a reduced overall level of basigin signal. Figure 4 shows representative sperm from the caput and cauda regions of WT and *Sept4*$^{-/-}$ mice. While basigin labels brightly in both WT caput and WT cauda sperm (Fig. 4, A and E, respectively), it can hardly be seen in images of *Sept4*$^{-/-}$ caput and cauda sperm (Fig. 4, B and F, respectively) taken with identical camera settings. The knockout sperm images have therefore been contrast-enhanced in Figure 4, C and G, to make the weak pattern more visible. Both sperm show a whole-membrane basigin distribution, including signal on the head, which was never observed in WT. Furthermore, the basigin presents on the knockout with a slightly uneven, patchy appearance and shows an additional reduction in label intensity between the caput and cauda stages. Figure 4, D and H, show similarly enhanced images of serum control sperm from *Sept4*$^{-/-}$ mice.

The majority (50%–70%) of the *Sept4*$^{-/-}$ sperm from the cauda region bend backward upon themselves at the site of their missing annulus (Fig. 4, F–H). This often made the basigin signal appear somewhat stronger within the midpiece, since the membrane is effectively doubled (Fig. 4G). To ascertain whether there is in fact any real concentration of signal within the midpiece of *Sept4*$^{-/-}$ cauda sperm, we looked specifically at the 30% of these sperm with straight tails. While there was no overall pattern of brighter labeling in the midpiece, we occasionally did observe individual sperm with a gradient of increasing signal intensity toward the proximal direction on the tail, including the midpiece, though without

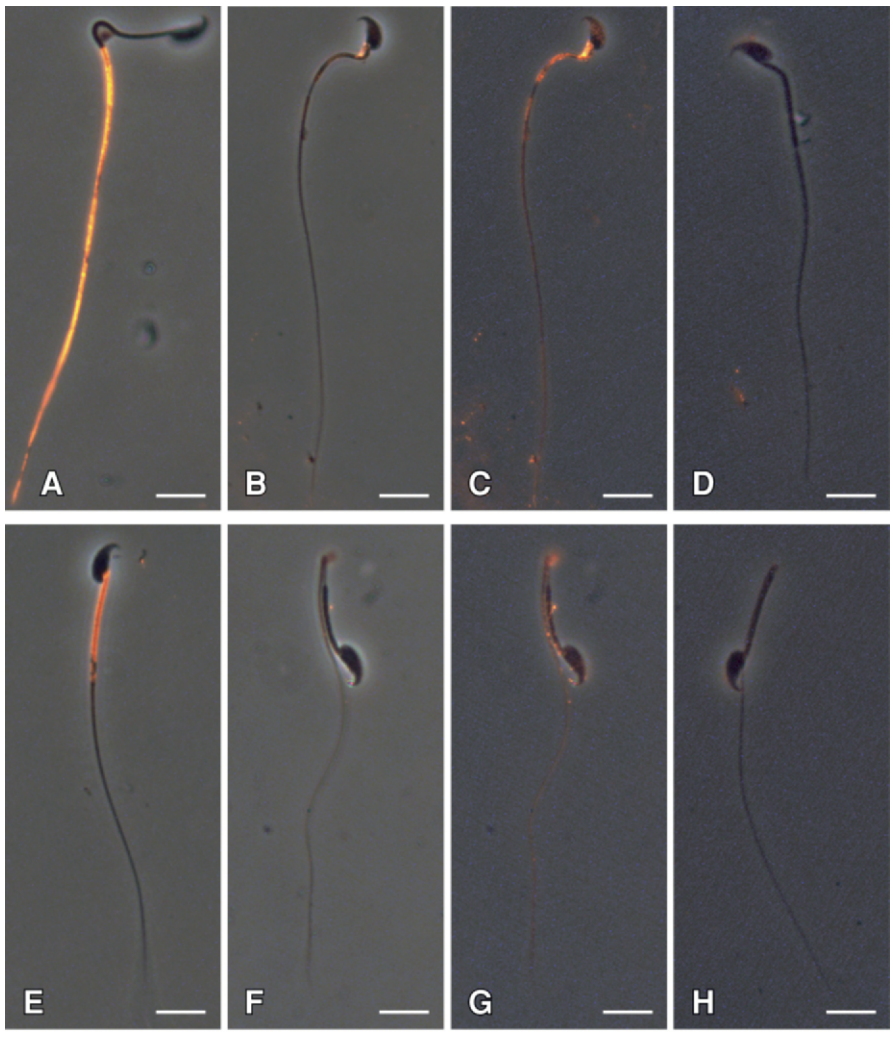

FIG. 4. Indirect immunofluorescent labeling of basigin on WT and *Sept4*$^{-/-}$ sperm. WT caput (**A**) and cauda (**E**) sperm show basigin localization within the principal piece and midpiece domains, respectively. Basigin is hardly detectable in *Sept4*$^{-/-}$ caput (**B**) and cauda (**F**) sperm at identical photographic exposures. Contrast enhancement of these images (**C** and **G**) reveals a weak and patchy basigin distribution over the whole membrane at both stages; **D** and **H** show similar enhancements of *Sept4*$^{-/-}$ sperm that served as serum controls. Micrographs are representative of findings from at least three experiments. Bar = 10 μm.

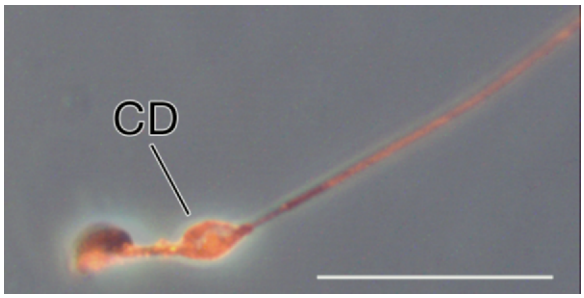

FIG. 5. Indirect immunofluorescent labeling of basigin on a caput sperm with a prominent cytoplasmic droplet (CD) from a *Sept4*$^{-/-}$ mouse. The image was taken with a different exposure time from those in Figure 4; thus, fluorescence intensity cannot be directly compared between the images. The image was contrast enhanced. Bar = 20 μm.

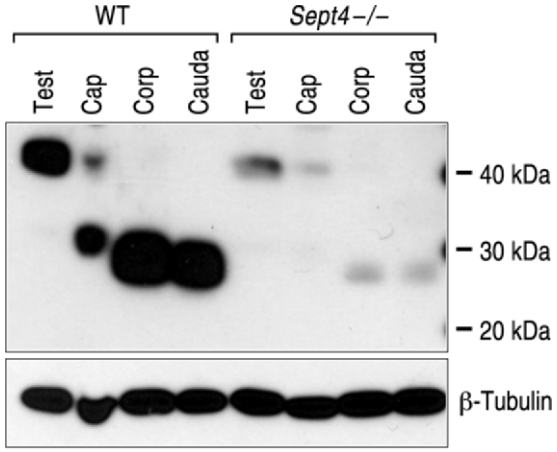

FIG. 6. Immunoblot showing reduced basigin levels in sperm from *Sept4*$^{-/-}$mice at various stages. Lanes consist of cell equivalent loads of sperm isolated from the testes (Test), as well as caput (Cap), corpus (Corp), and cauda regions of the epididymides of WT and *Sept4*$^{-/-}$ mice and visualized for basigin. Basigin undergoes proteolytic cleavage on caput sperm, leading to increased signal detection of the lower molecular weight form with the polyclonal antibody. The blot was stripped and reprobed for β-tubulin to confirm the loads. The figure is representative of results obtained from three separate experiments.

the clear boundary that is present in WT sperm (image not shown).

Finally, we detected one additional site of basigin localization on caput sperm from *Sept4*$^{-/-}$ mice: we saw prominent labeling of the cytoplasmic droplet (CD), whenever this remnant was observed (the cytoplasmic droplet is a small bleb of membrane and cytoplasm left after the residual body pinches off—it is subsequently shed, usually within the epididymis). A small CD can be seen labeling near the neck of the *Sept4*$^{-/-}$ sperm in Figure 4, B and C, and another slightly more distally along the midpiece in Figure 5. No similar labeling was observed on the CDs of WT caput sperm (Fig. 4A).

Reduced Basigin Levels in Annulus-Lacking Sperm Confirmed by Immunoblotting

To determine whether sperm from the *Sept4*$^{-/-}$ mice actually possess less basigin than sperm from WT animals, we performed immunoblots. We used the polyclonal rabbit serum antibody to probe for basigin on extracts of sperm isolated from the testes and from the caput, corpus, and cauda regions of the epididymides of both genotypes of mice. Figure 6 shows a representative immunoblot showing the diminution of basigin signal at all stages of sperm from the *Sept4*$^{-/-}$ animals, beginning with a several-fold difference on testicular sperm compared to WT. As is evident, basigin is subject to proteolytic cleavage in the early epididymis, going from a 40 kDa form on testicular sperm to one of about 27 kDa on cauda sperm [15, 18]. Concomitant with this proteolysis, we detected a substantial additional reduction in basigin signal on the sperm from the *Sept4*$^{-/-}$ mice, even though cleavage of basigin increased the sensitivity of its detection by the polyclonal antibody as seen in the WT lanes. The immunoblots were stripped and reprobed for tubulin to confirm that cell-equivalent loadings were achieved.

Redistribution and Loss of Basigin during Spermiogenesis in Annulus-Lacking Spermatids

We next sought to determine whether the reduced basigin levels in sperm from *Sept4*$^{-/-}$ mice resulted from a lower level of synthesis during spermatogenesis or a loss of protein at some step during sperm development. We performed immunohistolabeling for basigin using the polyclonal rabbit serum antibody on sections from paraffin-embedded, fixed testes from WT and *Sept4*$^{-/-}$ mice. The WT cross section (Fig. 7A) shows relatively strong basigin labeling within the tubules, although in differing patterns, presumably resulting from the differing maturational stages of the tubules depicted. The *Sept4*$^{-/-}$ cross section (Fig. 7B) shows similar labeling intensities and distribution patterns in several of the tubules, but very weak labeling in others. Negative serum controls were devoid of signal in both cases (Fig. 7, C and D).

In order to ascertain which step of spermiogenesis gave each labeling pattern, we conducted hematoxylin and eosin staining on serially ordered sections to each labeled section (images not shown) and staged tubules producing different labeling patterns. We found that basigin was initially expressed and distributed similarly for both genotypes. Both WT and *Sept4*$^{-/-}$ tissues demonstrated bright staining in round vesicles within the cytoplasm of elongating spermatids beginning about step 10 of spermiogenesis, within stage X seminiferous tubules (image not shown). These vesicles soon began to merge onto the tails of the spermatids, creating a patchy, whole tail pattern seen in steps 13 through early 15 (stages I–IV) for both genotypes (Fig. 8, A and a vs. D and d). However, during mid- to late step 15 (stages V–VI), as WT sperm experienced a further compartmentalization of basigin within the principal piece of the sperm tail (Fig. 8, B and b), sperm from *Sept4*$^{-/-}$ mice exhibited a diffuse basigin labeling pattern that moved off of the tail and out over the entire spermatid plasma membrane (Fig. 8, E and e). By step 16 of spermiogenesis (stages VII–VIII), the WT sperm exhibited bright and uniform, principal-piece only labeling of the sperm tail (Fig. 8, C and c), while *Sept4*$^{-/-}$ sperm showed dramatically less overall basigin labeling that was not confined to the sperm tail (Fig. 8, F and f).

Timing of Annulus Migration down the Axoneme in WT Spermatids

We hypothesized that the diffusion of basigin out from the tail of the *Sept4*$^{-/-}$ spermatid, at the exact time when it should have become confined within the principal piece domain, is a direct result of the missing annulus, which is needed for a diffusion barrier at this point. Therefore, we followed the biogenesis of the annulus in WT spermatids by immunohistolabeling testis sections, using septin 4 as our marker. We first

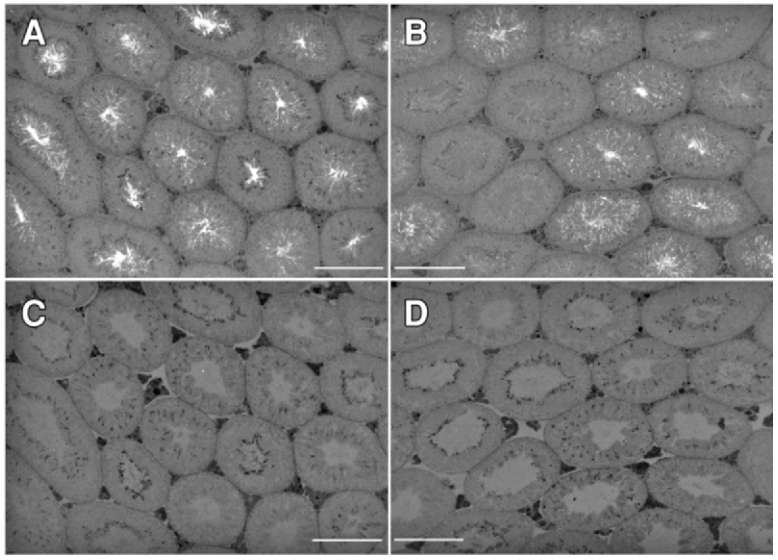

FIG. 7. Indirect immunofluorescent labeling of basigin on testicular tissue sections from WT (**A**) and *Sept4*$^{-/-}$ (**B**) mice, along with serum controls (**C** and **D**, respectively). Bar = 200 μm.

detected the developing annulus, weakly, on early step 10 spermatids (tubule stage X), which is around the time the annulus is first known to form [44, 45]. The labeling was dim but specific, appearing at the base of the sperm head next to the developing axoneme. The signal became brighter as the spermatids matured through the next several steps, while its position remained at the base of the head through step 14 (stage II–III; Fig. 9, A and D). During step 15 of spermatid development (which lasts from stages IV–VI), the position of the annulus shifted, moving from the head-neck region downward along the tail's midpiece (Fig. 9, B and E). The annulus came to rest at the midpiece-principal piece junction, in mid- to late step 15 of spermatid development. Figure 9, C and F, show the annulus at its final position on step 16 sperm (stage VII) shortly prior to their release into the lumen. Late step 15 is the same point we saw basigin lose confinement, move off the tail, and disperse over the entire plasma membrane of *Sept4*$^{-/-}$ sperm that have no annulus.

DISCUSSION

Using the diffusing membrane protein basigin to monitor domain integrity, we showed that in sperm without an annulus, the diffusion barrier between the principal piece and midpiece membrane domains indeed is lost. Furthermore, we established that basigin distribution on these sperm is first disordered at the very stage in spermiogenesis when the annulus normally completes its migration to its final position on the sperm tail. Together these findings suggest that the annulus has a direct role in restricting diffusion of membrane proteins on sperm.

Because the annulus is cytoskeletal, its precise function in establishing the membrane barrier is likely as a scaffold to which transmembrane proteins can adhere in a densely packed fashion. Such proteins could then act as a ''fence'' to keep basigin, and presumably other diffusing proteins, corralled within either the principal piece or midpiece membrane domain. This idea is supported by freeze-fracture analysis of the membrane directly over the annulus, which shows circumferential rows of tightly aligned particles (presumably transmembrane proteins) visible on the E-face of the membrane [19, 20, 46–48]. One transmembrane protein, Tat1, an anion transporter, has also been localized to the membrane directly over the annulus, and it has been suggested that it binds this structure and thus could participate in such a fence [49].

The annulus may also define and maintain lipids domains, and lipids might participate in establishing the barrier as well. The principal components of the annulus are septins, and many of the septin family members, including septin 4, have lipid-binding domains that can establish connections with the lipid bilayer [24, 42, 50–53]. Selvaraj et al. [10, 54] showed that the ganglioside G_{M1} strongly labels the membrane over the annulus and demonstrates a high level of domain retention in various membrane domains, including the midpiece of mouse sperm. A very similar pattern of G_{M1} labeling is also seen in bull sperm [55]. The *Sept4*$^{-/-}$ mouse, therefore, will likely be a useful tool in understanding the role lipids play in the creation and segregation of the domains centered around the annulus as well.

Interestingly, in Figure 2C, we show that a simple freeze-thaw of WT cauda sperm alters the boundary of basigin distribution such that it spreads into the membrane directly over the annulus. Although the barrier edge abutting the midpiece became permeable, the barrier remained intact at its distal edge, preventing basigin's diffusion into the principal piece. Whether the disruption of the barrier by freezing and thawing affects lipids or proteins is not known, but it suggests the barrier is not a uniform structure.

The hypothesis of a protein fence adherent to the annulus needs to be expanded to explicate how proteins such as basigin traverse this barrier and translocate from the principal piece to the midpiece. The annulus is a superstructure of septins, which, in other systems, can bind signaling as well as structural proteins [56–65]. We posit that an external signal could trigger a posttranslational modification of the annulus or attached membrane proteins, effectively opening a one-way gate in the membrane fence. A similar one-way transport of proteins occurs in yeast between the mother cell and the budding daughter cell, with a septin ring at the bud site selectively preventing a reflux of proteins back into the mother [36–39, 41]. A similar diffusion barrier has also been noted likewise at mammalian cleavage furrows [40].

Like basigin, PT-1 is also a freely diffusing membrane protein on the sperm tail that moves from the principal piece to the midpiece domain as shown on guinea pig sperm [3]. However, while basigin relocates within the epididymis, PT-1 does not traverse the annulus until capacitation. This suggests the annular barrier selectively allows specific proteins to translocate at specific times. Unfortunately, the sequence of

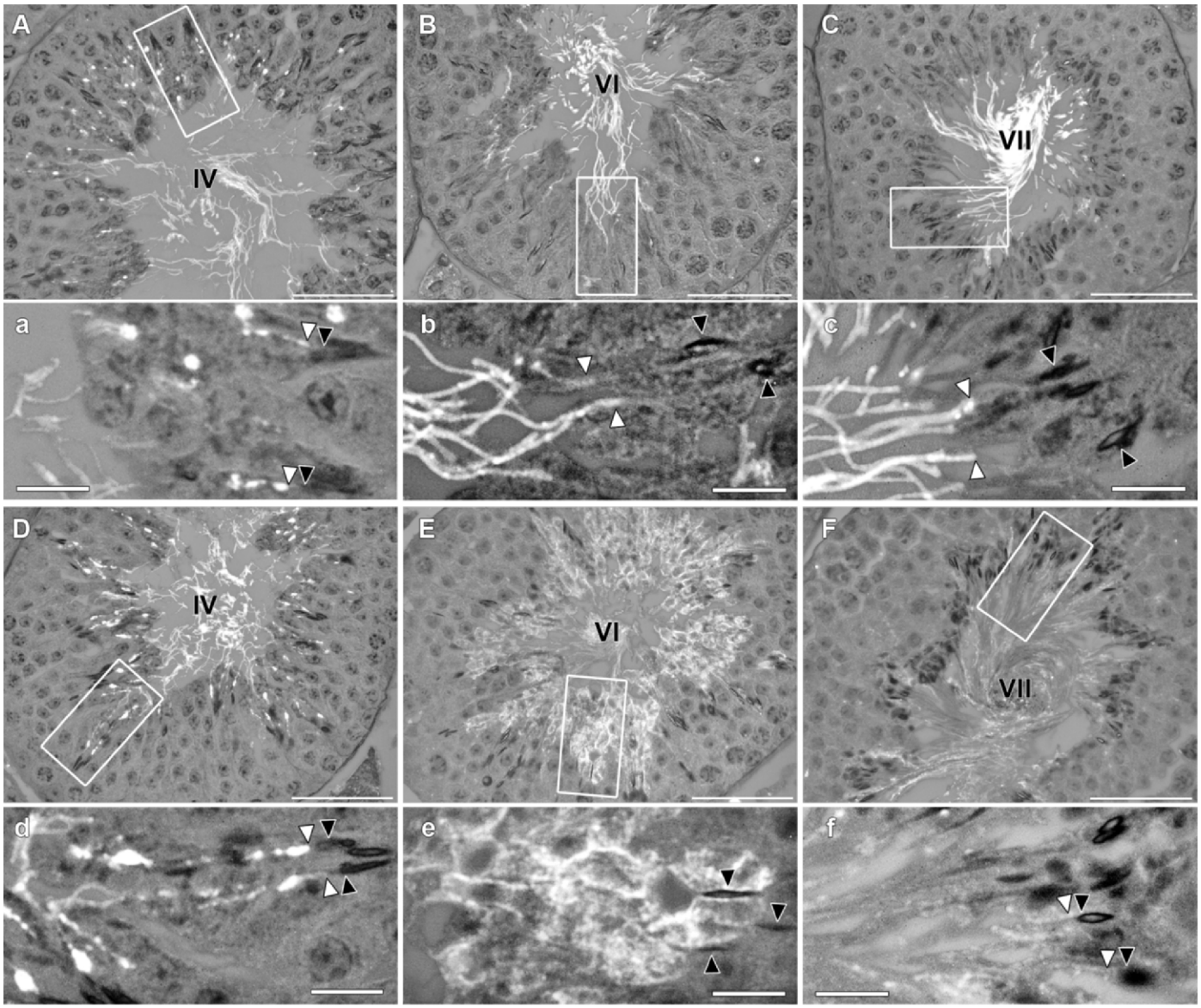

FIG. 8. Testicular cross sections labeled for basigin using indirect immunofluorescence. Micrographs depict tubules from WT (**A**–**C**) and *Sept4*$^{-/-}$ (**D**–**F**) mice, along with magnifications (**a**–**f**) of regions within the tubules (white rectangles) showing developing spermatids. Tubule stages are indicated by roman numerals. Black arrowheads point to sperm heads, and white arrowheads point to basigin on corresponding sperm tails. Bars = 50 μm (**A**–**F**) and 10 μm (**a**–**f**).

PT-1 is unknown, and the antibody that recognizes this guinea pig protein does not cross-react on mouse sperm, preventing us from testing this supposition with the *Sept4*$^{-/-}$ mice. Thus, the mechanisms that permit discriminate protein redistribution remain unclear.

During capacitation, basigin undergoes a second migration on WT sperm, moving from the midpiece onto the sperm head [18]. We saw basigin present on the heads of sperm from *Sept4*$^{-/-}$ mice beginning as early in development as isolated testicular and caput sperm. This is suggestive of a possible second barrier at the head/tail junction that is either septin dependent, and thus absent entirely in *Sept4*$^{-/-}$ mice, or is simply not active at these early stages before basigin would normally have moved into the midpiece.

We were intrigued by the finding that basigin is initially targeted to, and retained within, the tail of developing spermatids, regardless of the presence of an annulus. We saw no difference in the testicular labeling for basigin between WT and *Sept4*$^{-/-}$ until midstep 15 of spermiogenesis, at which time basigin redistributed to cover the entire plasma membrane of sperm from *Sept4*$^{-/-}$ mice. We showed that this correlates with the timing in WT mice when the annulus takes up its final position at the midpiece-principal piece junction. These findings agree with the results of a recent report on the biogenesis of the annulus in mice [45]. To explain these events, we suggest that when basigin is initially targeted to the tail, it may be held immobilized, so it cannot latterly diffuse. This putative anchoring would only be necessary until the annulus reaches the midpiece-principal piece boundary and establishes a membrane diffusion barrier. At this point, if basigin became freely diffusing, it would be retained within the principal piece by the diffusion barrier. In the annulus-lacking sperm, however, no diffusion barrier is established, and so if basigin is released from constraint, it would laterally diffuse over the entire plasma membrane of the developing spermatid, producing a pattern like that seen in Figure 8E. Interestingly, we did

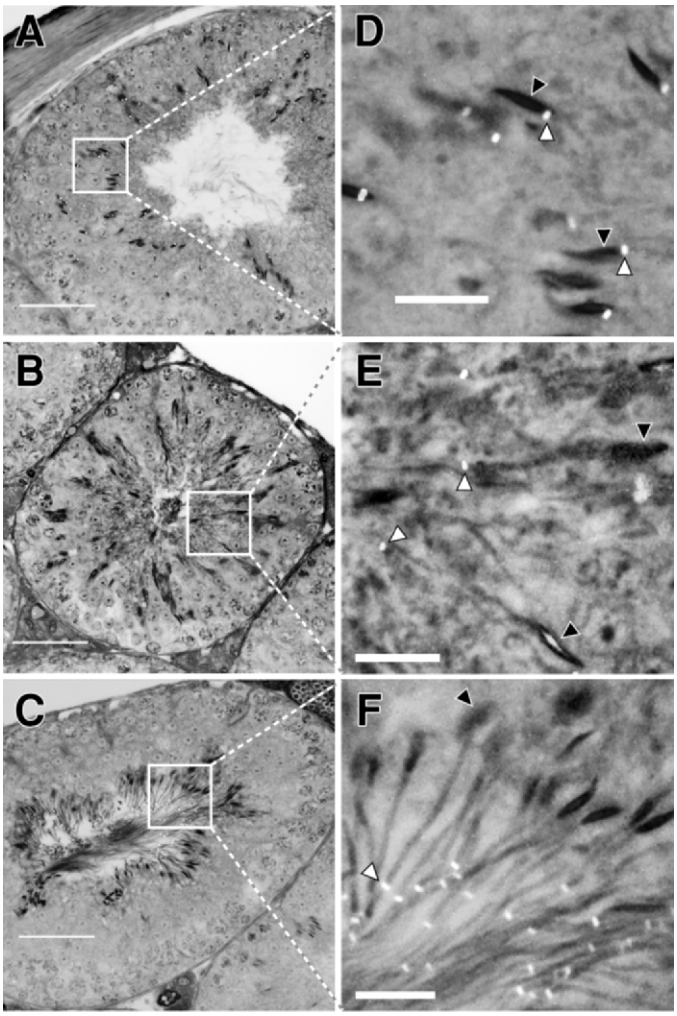

FIG. 9. Indirect immunofluorescent labeling of the annular protein septin 4 on testicular tissue sections from WT mice showing annulus migration during spermiogenesis. The micrographs depict seminiferous tubules at stages II–III (**A**), IV–V (**B**), and VII–VIII (**C**) of the cycle and a region within each tubule (the white boxes) that has been magnified to show detail on the elongating spermatids. On step 14 spermatids (**D**), the annuli appear at the base of the condensed nuclei. During step 15 of spermatid development (**E**), the annuli migrate down the length of the midpiece. At step 16 (**F**), the annuli are seen at the midpiece-principal piece junction. White arrowheads point to the labeled annulus and black arrowheads point to the corresponding sperm heads. Bars = 50 μm (**A**–**C**) and 10 μm (**D**–**F**).

observe principal piece domain restriction in about 5% of caput sperm from *Sept4*$^{-/-}$ mice (Table 1). If basigin is initially immobilized on the tails of developing spermatids, then this population might represent sperm on which basigin failed to become freely diffusing. Precedence for a change in the diffusion coefficient for a sperm protein is seen with the heterodimeric sperm protein ADAM1/ADAM2 (fertilin). We previously showed that ADAM1/ADAM2 alters from an anchored state to a freely diffusing state, in this case, at the time the sperm undergoes capacitation [5, 8].

An unexpected consequence of not having the annulus was a significant loss of basigin from the sperm. Sequestering proteins within a membrane domain may not only serve to position them at the right place and time for proper function, but it could also protect them from unwanted loss. The sperm proteins ADAM1/ADAM2 and SPAM1 are membrane proteins that redistribute from covering the whole sperm head to being strictly confined within the posterior head domain during epididymal maturation [3, 4, 12]. These proteins have functional importance after the acrosome reaction; therefore, if they were not confined to the posterior head domain, a significant loss of these proteins would occur when the anterior head membrane is shed during the acrosome reaction. We showed that the sequestration of basigin in the principal piece during late spermiogenesis is necessary to protect it from loss.

The loss of basigin in the *Sept4*$^{-/-}$ sperm appeared to occur at two major points. The first loss occurred just prior to sperm release into the lumen of the seminiferous tubules. Presumably, basigin that had moved onto the plasma membrane not belonging to the final sperm was internalized and degraded, or otherwise pinched off and discarded on the residual body during spermiation.

The second loss occurred during epididymal maturation and roughly correlated with both the proteolytic cleavage of basigin and the sloughing of the cytoplasmic droplet (CD). Given that a strong basigin presence was often observed in the CDs of *Sept4*$^{-/-}$ (but not WT) caput sperm, it is reasonable that the CD may be a source of protein loss in the knockout. The CD is normally shed from WT sperm before basigin relocates, thus avoiding this potential loss of the protein. The proteolytic cleavage of basigin while in a whole membrane distribution on the *Sept4*$^{-/-}$ sperm may also contribute to its loss, but the mechanism remains unknown.

The results establish that the sperm annulus is essential for generating the diffusion barrier that separates the midpiece and principal piece membrane domains. Significantly, they are the most compelling direct evidence to date of a septin structure performing this function in mammalian cells. Our data also demonstrate that the putative transmembrane protein barricade is not engaged until the annulus finishes its migrations down the tail to the principal piece-midpiece junction. Thus, the annulus may need to be at its final position before a diffusion barrier can be established. Therefore, an alternative mechanism (such as anchoring) is needed to hold diffusible proteins within their tail domain until the annulus-dependent diffusion barrier is established. Finally, investigating the annulus as a diffusion barrier will continue to affect our understanding of how this organelle is critical to fertility not only in mice but in men seeking clinical treatment for annulus-related cases of asthenozoospermic infertility [22, 23, 66, 67].

ACKNOWLEDGMENTS

We gratefully thank Dr. Herman Steller for providing us with the *Sept4*$^{-/-}$ mice and Dr. James Bartles for giving us anti-CE9 (basigin) polyclonal antibody. We also want to thank Mr. Evan Read for his illustrative work and his assistance in the preparation of the manuscript.

REFERENCES

1. Monesi V. Synthetic activities during spermatogenesis in the mouse. Exp Cell Res 1965; 39:197–224.
2. Cowan AE, Primakoff P, Myles DG. Sperm exocytosis increases the amount of PH-20 antigen on the surface of guinea pig sperm. J Cell Biol 1986; 103:1289–1297.
3. Myles DG, Koppel DE, Cowan AE, Phelps BM, Primakoff P. Rearrangement of sperm surface antigens prior to fertilization. Ann N Y Acad Sci 1987; 513:262–273.
4. Hunnicutt GR, Koppel DE, Myles DG. Analysis of the process of localization of fertilin to the sperm posterior head plasma membrane domain during sperm maturation in the epididymis. Dev Biol 1997; 191: 146–159.
5. Cowan AE, Koppel DE, Vargas LA, Hunnicutt GR. Guinea pig fertilin exhibits restricted lateral mobility in epididymal sperm and becomes freely diffusing during capacitation. Dev Biol 2001; 236:502–509.
6. Christova Y, James PS, Cooper TG, Jones R. Lipid diffusion in the plasma

membrane of mouse spermatozoa: changes during epididymal maturation, effects of pH, osmotic pressure, and knockout of the c-ros gene. J Androl 2002; 23:384–392.
7. Christova Y, James P, Mackie A, Cooper TG, Jones R. Molecular diffusion in sperm plasma membranes during epididymal maturation. Mol Cell Endocrinol 2004; 216:41–46.
8. Hunnicutt GR, Koppel DE, Kwitny S, Cowan AE. Cyclic 3′,5′-AMP causes ADAM1/ADAM2 to rapidly diffuse within the plasma membrane of guinea pig sperm. Biol Reprod 2008; 79:999–1007.
9. Gadella BM, Tsai PS, Boerke A, Brewis IA. Sperm head membrane reorganisation during capacitation. Int J Dev Biol 2008; 52:473–480.
10. Selvaraj V, Asano A, Buttke DE, Sengupta P, Weiss RS, Travis AJ. Mechanisms underlying the micron-scale segregation of sterols and GM1 in live mammalian sperm. J Cell Physiol 2009; 218:522–536.
11. Miranda PV, Allaire A, Sosnik J, Visconti PE. Localization of low-density detergent-resistant membrane proteins in intact and acrosome-reacted mouse sperm. Biol Reprod 2009; 80:897–904.
12. Myles DG, Primakoff P. Localized surface antigens of guinea pig sperm migrate to new regions prior to fertilization. J Cell Biol 1984; 99:1634–1641.
13. Phelps BM, Koppel DE, Primakoff P, Myles DG. Evidence that proteolysis of the surface is an initial step in the mechanism of formation of sperm cell surface domains. J Cell Biol 1990; 111:1839–1847.
14. Myles DG, Primakoff P, Koppel DE. A localized surface protein of guinea pig sperm exhibits free diffusion in its domain. J Cell Biol 1984; 98:1905–1909.
15. Petruszak JA, Nehme CL, Bartles JR. Endoproteolytic cleavage in the extracellular domain of the integral plasma membrane protein CE9 precedes its redistribution from the posterior to the anterior tail of the rat spermatozoon during epididymal maturation. J Cell Biol 1991; 114:917–927.
16. Nehme CL, Cesario MM, Myles DG, Koppel DE, Bartles JR. Breaching the diffusion barrier that compartmentalizes the transmembrane glycoprotein CE9 to the posterior-tail plasma membrane domain of the rat spermatozoon. J Cell Biol 1993; 120:687–694.
17. Cesario MM, Bartles JR. Compartmentalization, processing and redistribution of the plasma membrane protein CE9 on rodent spermatozoa. Relationship of the annulus to domain boundaries in the plasma membrane of the tail. J Cell Sci 1994; 107(Pt 2):561–570.
18. Saxena DK, Oh-Oka T, Kadomatsu K, Muramatsu T, Toshimori K. Behaviour of a sperm surface transmembrane glycoprotein basigin during epididymal maturation and its role in fertilization in mice. Reproduction 2002; 123:435–444.
19. Elias PM, Goerke J, Friend DS, Brown BE. Freeze-fracture identification of sterol-digitonin complexes in cell and liposome membranes. J Cell Biol 1978; 78:577–596.
20. Fawcett D, Bedford J (eds.). The Spermatozoon: Maturation, Motility, Surface Properties and Comparative Aspects. Baltimore: Urban & Schwarzenberg; 1979.
21. Igakura T, Kadomatsu K, Kaname T, Muramatsu H, Fan QW, Miyauchi T, Toyama Y, Kuno N, Yuasa S, Takahashi M, Senda T, Taguchi O, Yamamura K, Arimura K, Muramatsu T. A null mutation in basigin, an immunoglobulin superfamily member, indicates its important roles in peri-implantation development and spermatogenesis. Dev Biol 1998; 194:152–165.
22. Ihara M, Kinoshita A, Yamada S, Tanaka H, Tanigaki A, Kitano A, Goto M, Okubo K, Nishiyama H, Ogawa O, Takahashi C, Itohara S, Nishimune Y, Noda M, Kinoshita M. Cortical organization by the septin cytoskeleton is essential for structural and mechanical integrity of mammalian spermatozoa. Dev Cell 2005; 8:343–352.
23. Kissel H, Georgescu MM, Larisch S, Manova K, Hunnicutt GR, Steller H. The Sept4 septin locus is required for sperm terminal differentiation in mice. Dev Cell 2005; 8:353–364.
24. Steels JD, Estey MP, Froese CD, Reynaud D, Pace-Asciak C, Trimble WS. Sept12 is a component of the mammalian sperm tail annulus. Cell Motil Cytoskeleton 2007; 64:794–807.
25. Field CM, Kellogg D. Septins: cytoskeletal polymers or signalling GTPases? Trends Cell Biol 1999; 9:387–394.
26. Kinoshita M, Noda M. Roles of septins in the mammalian cytokinesis machinery. Cell Struct Funct 2001; 26:667–670.
27. Mitchison TJ, Field CM. Cytoskeleton: what does GTP do for septins? Curr Biol 2002; 12:R788–790.
28. Field CM, al-Awar O, Rosenblatt J, Wong ML, Alberts B, Mitchison TJ. A purified Drosophila septin complex forms filaments and exhibits GTPase activity. J Cell Biol 1996; 133:605–616.
29. Frazier JA, Wong ML, Longtine MS, Pringle JR, Mann M, Mitchison TJ, Field C. Polymerization of purified yeast septins: evidence that organized filament arrays may not be required for septin function. J Cell Biol 1998; 143:737–749.
30. Mendoza M, Hyman AA, Glotzer M. GTP binding induces filament assembly of a recombinant septin. Curr Biol 2002; 12:1858–1863.
31. Hartwell LH, Culotti J, Pringle JR, Reid BJ. Genetic control of the cell division cycle in yeast. Science 1974; 183:46–51.
32. Hartwell LH, Hutchison HT, Holland TM, McLaughlin CS. The effect of cycloheximide upon polyribosome stability in two yeast mutants defective respectively in the initiation of polypeptide chains and in messenger RNA synthesis. Mol Gen Genet 1970; 106:347–361.
33. Hartwell LH, Culotti J, Reid B. Genetic control of the cell-division cycle in yeast. I. Detection of mutants. Proc Natl Acad Sci U S A 1970; 66:352–359.
34. Hartwell LH. Macromolecule synthesis in temperature-sensitive mutants of yeast. J Bacteriol 1967; 93:1662–1670.
35. Byers B, Goetsch L. A highly ordered ring of membrane-associated filaments in budding yeast. J Cell Biol 1976; 69:717–721.
36. Gladfelter AS, Pringle JR, Lew DJ. The septin cortex at the yeast mother-bud neck. Curr Opin Microbiol 2001; 4:681–689.
37. Takizawa PA, DeRisi JL, Wilhelm JE, Vale RD. Plasma membrane compartmentalization in yeast by messenger RNA transport and a septin diffusion barrier. Science 2000; 290:341–344.
38. Faty M, Fink M, Barral Y. Septins: a ring to part mother and daughter. Curr Genet 2002; 41:123–131.
39. Luedeke C, Frei SB, Sbalzarini I, Schwarz H, Spang A, Barral Y. Septin-dependent compartmentalization of the endoplasmic reticulum during yeast polarized growth. J Cell Biol 2005; 169:897–908.
40. Schmidt K, Nichols BJ. A barrier to lateral diffusion in the cleavage furrow of dividing mammalian cells. Curr Biol 2004; 14:1002–1006.
41. Caudron F, Barral Y. Septins and the lateral compartmentalization of eukaryotic membranes. Dev Cell 2009; 16:493–506.
42. Buser AM, Erne B, Werner HB, Nave KA, Schaeren-Wiemers N. The septin cytoskeleton in myelinating glia. Mol Cell Neurosci 2009; 40:156–166.
43. Travis AJ, Merdiushev T, Vargas LA, Jones BH, Purdon MA, Nipper RW, Galatioto J, Moss SB, Hunnicutt GR, Kopf GS. Expression and localization of caveolin-1, and the presence of membrane rafts, in mouse and guinea pig spermatozoa. Dev Biol 2001; 240:599–610.
44. Fawcett DW, Eddy EM, Phillips DM. Observations on the fine structure and relationships of the chromatoid body in mammalian spermatogenesis. Biol Reprod 1970; 2:129–153.
45. Guan J, Kinoshita M, Yuan L. Spatiotemporal association of DNAJB13 with the annulus during mouse sperm flagellum development. BMC Dev Biol 2009; 9:23.
46. Kan FW, Pinto da Silva P. Molecular demarcation of surface domains as established by label-fracture cytochemistry of boar spermatozoa. J Histochem Cytochem 1987; 35:1069–1078.
47. Kan FW, Lin Y. Topographical distribution of phospholipids in boar sperm plasma and intracellular membranes as revealed by freeze-fracture cytochemistry. J Histochem Cytochem 1996; 44:687–701.
48. Friend DS, Elias PM, Rudolf I. Disassembly of the guinea pig sperm tail. In: Fawcett DW, Bedford JM (eds.), The Spermatozoon: Maturation, Motility, Surface Properties and Comparative Aspects. Baltimore: Urban & Schwarzenberg; 1979:157–172.
49. Touré A, Lhuillier P, Gossen JA, Kuil CW, Lhote D, Jegou B, Escalier D, Gacon G. The testis anion transporter 1 (Slc26a8) is required for sperm terminal differentiation and male fertility in the mouse. Hum Mol Genet 2007; 16:1783–1793.
50. Zhang J, Kong C, Xie H, McPherson PS, Grinstein S, Trimble WS. Phosphatidylinositol polyphosphate binding to the mammalian septin H5 is modulated by GTP. Curr Biol 1999; 9:1458–1467.
51. Casamayor A, Snyder M. Molecular dissection of a yeast septin: distinct domains are required for septin interaction, localization, and function. Mol Cell Biol 2003; 23:2762–2777.
52. Tanaka-Takiguchi Y, Kinoshita M, Takiguchi K. Septin-mediated uniform bracing of phospholipid membranes. Curr Biol 2009; 19:140–145.
53. Beh CT, Alfaro G, Duamel G, Sullivan DP, Kersting MC, Dighe S, Kozminski KG, Menon AK. Yeast oxysterol-binding proteins: sterol transporters or regulators of cell polarization? Mol Cell Biochem 2009; 326:9–13.
54. Selvaraj V, Buttke DE, Asano A, McElwee JL, Wolff CA, Nelson JL, Klaus AV, Hunnicutt GR, Travis AJ. GM1 dynamics as a marker for membrane changes associated with the process of capacitation in murine and bovine spermatozoa. J Androl 2007; 28:588–599.
55. Buttke DE, Nelson JL, Schlegel PN, Hunnicutt GR, Travis AJ. Visualization of GM1 with cholera toxin B in live epididymal versus

ejaculated bull, mouse, and human spermatozoa. Biol Reprod 2006; 74: 889–895.
56. Sanders SL, Herskowitz I. The BUD4 protein of yeast, required for axial budding, is localized to the mother/BUD neck in a cell cycle-dependent manner. J Cell Biol 1996; 134:413–427.
57. Chant J, Mischke M, Mitchell E, Herskowitz I, Pringle JR. Role of Bud3p in producing the axial budding pattern of yeast. J Cell Biol 1995; 129:767–778.
58. Chant J, Pringle JR. Patterns of bud-site selection in the yeast Saccharomyces cerevisiae. J Cell Biol 1995; 129:751–765.
59. Chant J, Stowers L. GTPase cascades choreographing cellular behavior: movement, morphogenesis, and more. Cell 1995; 81:1–4.
60. Pringle JR, Bi E, Harkins HA, Zahner JE, De Virgilio C, Chant J, Corrado K, Fares H. Establishment of cell polarity in yeast. Cold Spring Harb Symp Quant Biol 1995; 60:729–744.
61. Bi E, Maddox P, Lew DJ, Salmon ED, McMillan JN, Yeh E, Pringle JR. Involvement of an actomyosin contractile ring in Saccharomyces cerevisiae cytokinesis. J Cell Biol 1998; 142:1301–1312.
62. Lippincott J, Li R. Sequential assembly of myosin II, an IQGAP-like protein, and filamentous actin to a ring structure involved in budding yeast cytokinesis. J Cell Biol 1998; 140:355–366.
63. DeMarini DJ, Adams AE, Fares H, De Virgilio C, Valle G, Chuang JS, Pringle JR. A septin-based hierarchy of proteins required for localized deposition of chitin in the Saccharomyces cerevisiae cell wall. J Cell Biol 1997; 139:75–93.
64. Longtine MS, Fares H, Pringle JR. Role of the yeast Gin4p protein kinase in septin assembly and the relationship between septin assembly and septin function. J Cell Biol 1998; 143:719–736.
65. Longtine MS, Theesfeld CL, McMillan JN, Weaver E, Pringle JR, Lew DJ. Septin-dependent assembly of a cell cycle-regulatory module in Saccharomyces cerevisiae. Mol Cell Biol 2000; 20:4049–4061.
66. Sugino Y, Ichioka K, Soda T, Ihara M, Kinoshita M, Ogawa O, Nishiyama H. Septins as diagnostic markers for a subset of human asthenozoospermia. J Urol 2008; 180:2706–2709.
67. Lhuillier P, Rode B, Escalier D, Lores P, Dirami T, Bienvenu T, Gacon G, Dulioust E, Touré A. Absence of annulus in human asthenozoospermia: case report. Hum Reprod 2009; 24(6):1296–1303.